PR12-18-002

Date: May 30, 2018

Be Target Assembly for KLF project: Conceptual Design

I. I. Strakovsky[1], M. J. Amaryan[2], W. J. Briscoe[1], P. Degtyarenko[3], A. Somov[3], J. R. Stevens[4], T. Whitlatch[3],

[1] The George Washington University, Washington, DC 20052, USA
[2] Old Dominion University, Norfolk, VA 23529, USA
[3] Thomas Jefferson National Accelerator Facility, Newport News, VA 23606, USA
[4] College of William and Mary, Williamsburg, VA 23185, USA

Abstract

A conceptual design of the Be target assembly for neutral kaon experiments [1] to be used with the GlueX experimental setup for strange hadron spectroscopy.

Contents

1 K_L Beam at Hall D

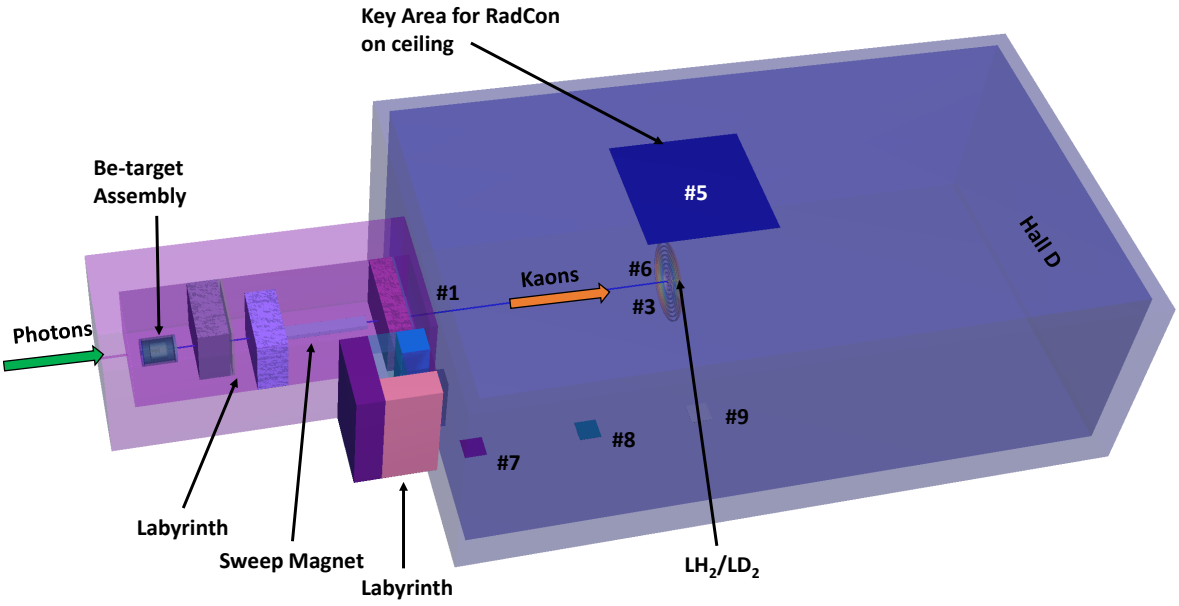

Figure 1: Schematic view of Hall D setting for MCNP transport code [2] calculations. Beam goes from left to right. The model is presented as semi-transparent for demonstration purposes. These 3D plots are a part of the Hall D beamline and some tallies are shown.

At the first stage 12 GeV electrons will scatter in the copper radiator (10% R.L.) inside the Compact Photon Source (CPS), generating an intense beam of untagged bremsstrahlung photons. The CPS will be located downstream of the tagger magnet. The tagger alcove has more space than that available in Halls A/C. So the positioning of the CPS and the placement of shielding are simplified. The Hall D tagger magnet and detectors will not be used. At the second stage, bremsstrahlung photons will hit the Be target assembly located at the beginning of the collimator cave (Fig. 1), and produce neutral kaons along with neutrons, photons, and charged particles. GlueX wiki [3] is a source of the collimator cave geometry. Additional shielding inside of the collimator cave was optimized to minimaize the neutron and gamma background in the experimental Hall D and to satisfy a RadCon requirement establishing the radiation dose rate limit in the experimental hall (1 mrem/h).

The beam tungsten plug is placed right after beryllium. Two concrete walls (the labyrinth) in the collimator cave will reduce neutron and photon background and allow access to the Be-target from the experimental hall are both 1.21 m thick and have 0.5 m gap between them (Fig. 2). The first concrete wall has additional 0.10 m lead shielding. The permanent sweeping magnet (3.83 m in length) is placed right after the second concrete wall. It cleans up the charged component of the beam and has a field integral of 0.8 Tm, which is enough to remove all charged background coming out of the Be-target assembly.

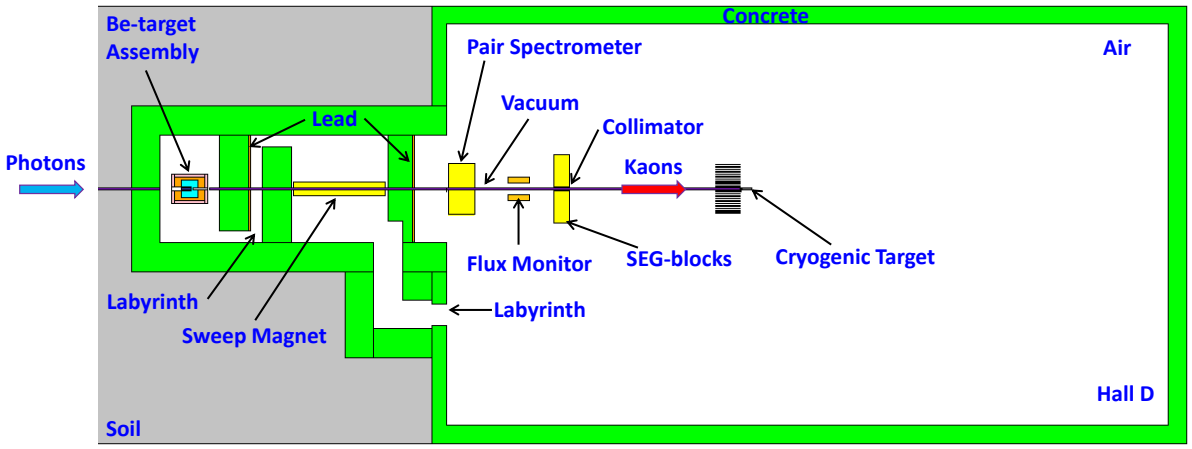

Figure 2: Schematic view of the collimator cave with the Be-target assemply (more details on Fig. 3) concrete wals, and sweeping magnet. Beam goes from left to right. The detail geometry of the collimator cave is given in Appendix 5.

The vacuum beam pipe has a ∅0.07 m and prevents neutron rescattering in air. Finally, K_L mesons will reach the LH_2/LD_2 cryogenic target located inside the GlueX spectrometer. The distance between the primary Be and cryogenic targets is 24 m. The flux of K_L mesons will be measured by a Flux Monitor (FM) [4] (1.2 m length) located in the experimental hall in just 2 m (it would utilize the K_L in-flight decays) behind the Pair Spectrometer [5].

2 Elements of the Be-target Assembly

Schematic view of the Be-target assembly (K_L production target) is given in Fig. 3. Lighter elements provide higher photoproduction yield for a unit of radiation length. Beryllium targets were used for KL production at SLAC [6] and NINA [7]. The beam tungsten plug of a 0.10 m thick (30 R.L.) absorbs the photon beam (Fig. 3).

Elements of the Be-target assembly are presented in Table 1. The weight of the construction is 14.5 ton. Changeover from the photon to the KL beamline and from the KL to the photon beamline requires further evaluation. However, initial conservative estimates are that this changeover could be completed approximately in 6 months. Therefore, the majority of this changeover could be completed during a typical summer shutdown period in the CEBAF accelerator schedule. It has to be mentioned that the collimator cave has enough space (with the 4.52 m width) for the Be-target

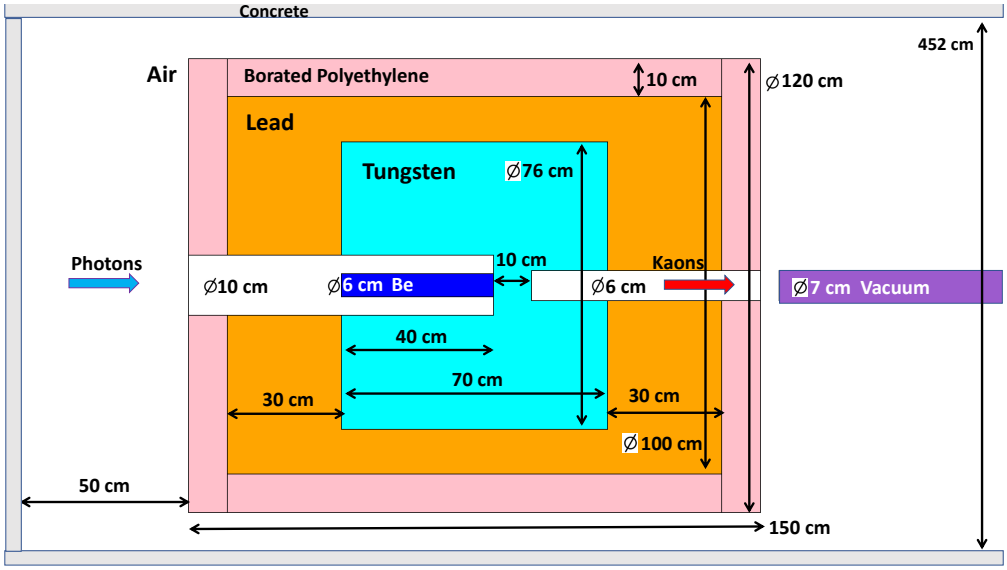

Figure 3: Schematic view of the Be-target (K_L production target) assembly. Concrete, borated polyethylene, lead, tungsten, beryllium, vacuum beam pipe, and air shown by grey, pink, brown, light blue, blue, violet, and white color, respectively. Beam goes from left to right.

assembly to remain far enough from the beamline. The detail geometry of the collimator cave is given in Appendix 5.

Water cooling would be required around the Be target and in the selected tungsten plug. Cooling water is available in the experimental hall that can be used to dissipate 6 kW of power delivered by the photon beam.

Table 1: Elements of the Be-target assembly.

Element	Outer ∅/Inner ∅ (m)	Thickness (m)	Volume (m^3)	Density (kg/m^3)	Mass (kg)
Borated polyethylen (front)	1.20/0.16	0.10	0.111	1000	111.1
Borated polyethylen (side)	1.20/1.00	1.30	0.449	1000	449.2
Borated polyethylen (back)	1.20/0.08	0.10	0.113	1000	112.6
Lead (front)	1.00/0.16	0.30	0.230	11350	2605.8
Lead (side)	1.00/0.76	0.70	0.232	11350	2635.8
Lead (back)	1.00/0.08	0.30	0.234	11350	2657.2
Tungsten (front)	0.76/0.16	0.40	0.173	19300	3346.9
Tungsten (center)	0.76/0.00	0.10	0.045	19300	875.5
Tungsten (back)	0.76/0.08	0.20	0.090	19300	1731.7
Beryllium	0.06/0.00	0.40	0.001	1848	2.1

3 Background Calculations

To estimate the neutron and gamma flux in a beam and neutron dose rate in the experimental hall from scattered neutrons and gamma, we used the MCNP6 N-Particle (MCNP) Transport code [2]. The realism of MCNP simulations is based on the advanced nuclear cross section libraries created and maintained in national laboratories of DOE complex. The physical models implemented in the MCNP6 code take into account bremsstrahlung photon production, photonuclear reactions, neutron and photons multiple scattering processes. The experimental hall, collimator cave, and photon beam resulted from tungsten radiator were modeled using the specifications from the layout presented in Figure 1 shown as a 3D graphic model of the experimental setup.

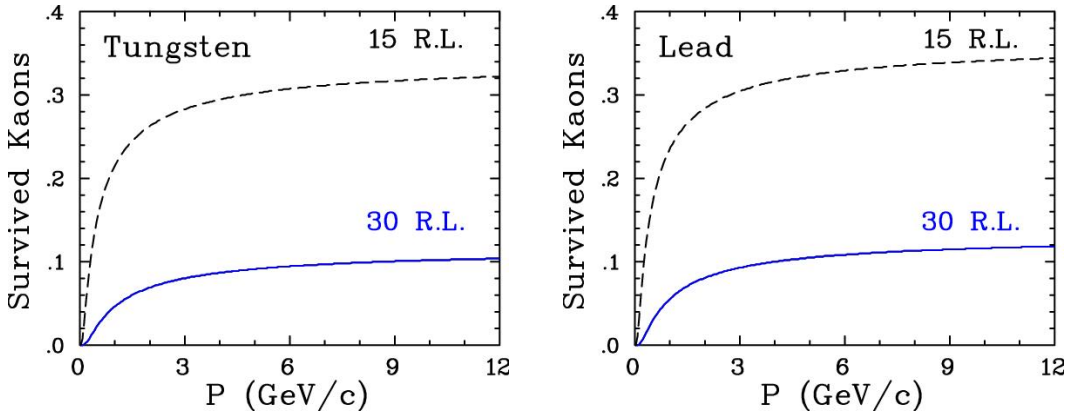

Figure 4: Fraction of survived kaons after the tungsten (left) or lead (right) plugs are installed with 15 or 30 R.L.

The MCNP model simulates a 12 GeV 5μA electron beam hitting the copper radiator inside the CPS. Electron transport was traced in copper radiator, vacuum beam pipe for bremsstrahlung photons, and Be-target. Neutrons and photons were traced in all components of the used MCNP model. The media outside concrete walls of the collimator cave and bremsstrahlung photon beam pipe was excluded from consideration to facilitate the calculations.

For MCNP calculations (in terms of flux [part/s/cm^2] or biological dose rate [mrem/h]), several tallies (as Tables 2 and 3 will show below) were placed along the beam and at the experimental hall for neutron and gamma fluence estimation. Fluence-to-Effective Dose conversion factors from ICRP 116 [8] were implemented to convert neutron fluence to effective dose rate.

Tally descriptions are:

- **#1**: spot for flux ($\varnothing$0.07 m) on the beam in the experimental hall right behind of the concrete wall;
- **#2**: spot for flux ($\varnothing$0.07 m) outside the beam in the experimental hall right behind of the concrete wall;
- **#3**: spot for flux ($\varnothing$0.07 m) on the beam in the experimental hall right on the face of the cryogenic target;

- **#4**: spot for flux (∅0.07 m) outside the beam in the experimental hall right on the face of the cryogenic target;
- **#5**: area for dose rate (6×6 m^2) on ceiling of the experimental hall centered at the GlueX detector - key area for the RadCon;
- **#6**: ring for dose rate (outer ∅0.08 m and inner ∅0.07 m) on the face of the cryogenic target - to evaluate a radiation damage for the SiPMs;
- **#7-9**: area for dose rate (1×1 m^2) hallway in the experimental hall following the GlueX detector;
- **#10-19**: rings for dose rate (outer ∅0.25, 0.45, 0.65, 0.85, 1.05, 1.25, 1.45, 1.65, 1.85, 2.05 m and inner ∅0.20, 0.40, 0.60, 0.80, 1.00, 1.20, 1.40, 1.60, 1.80, 2.00 m, respectively) on the face of the cryogenic target - to evaluate a radiation damage for the front of the BCAL;
- **#20**: spot for flux (∅0.07 m) on the beam right behind beryllium;
- **#21**: spot for flux (∅0.07 m) on the beam right behind tungsten.

K_Ls, produced by the Be-target and survived after the beam tungsten or lead plug, are presented in Fig. 4. This figure shows that there is a small effect in the material difference in the beam plug. There are 10% of K_Ls, produced by the Be-target, survived after the beam tungsten plug. The neutron yield integral from the berilium is $2.4 \times 10^{10}\ n/(s \cdot cm^2)$ and then from tunsten is $4.2 \times 10^{9}\ n/(s \cdot cm^2)$ (Figs. 5 and 6). So, the tungsten plug reduced the neutron flux by the same amount as the neutral kaon flux.

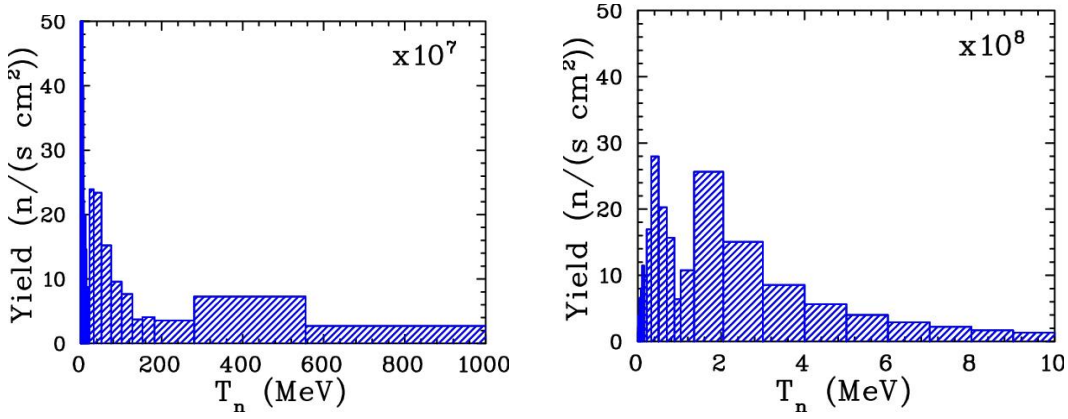

Figure 5: Number of neutrons that will not pass through tungsten. Calculations were performed using the MCNP Transport code [2].

3.1 Neutron Background

Calculations were performed for different shielding configurations in the collimator cave to minimize the neutron and gamma dose rate. The vertical (horizontal) cross section of the neutron flux is given in Fig. 7 (Fig. 8).

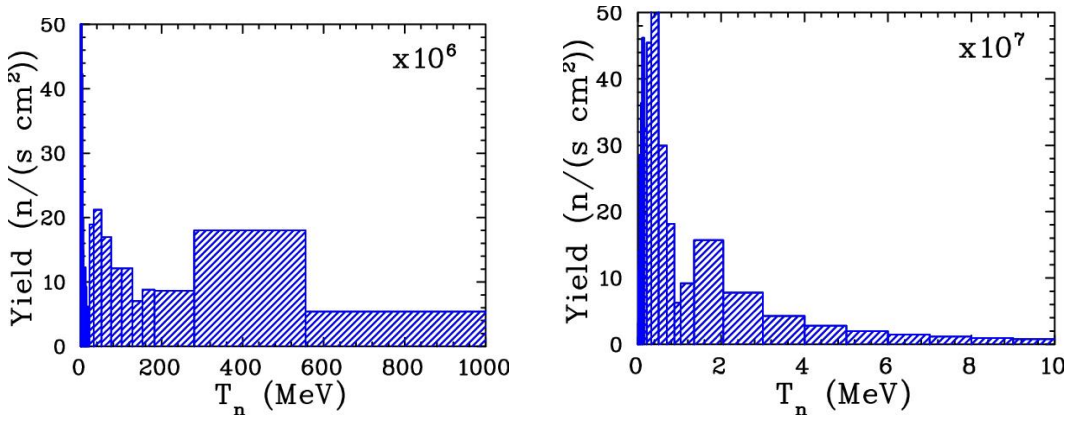

Figure 6: Number of neutrons that will pass through tungsten. Calculations were performed using the MCNP Transport code [2].

The tally #5 (Table 3) was selected by RadCon to estimate neutron fluence at the experimental hall ceiling just above the GlueX detector. That is the Key Area for RadCon shown in Fig. 1. The neutron dose rate calculated for the layouts from Figs. 7 and 8 on tally #5 is 0.11 ± 0.04 mrem/h. It is acceptable by RadCon.

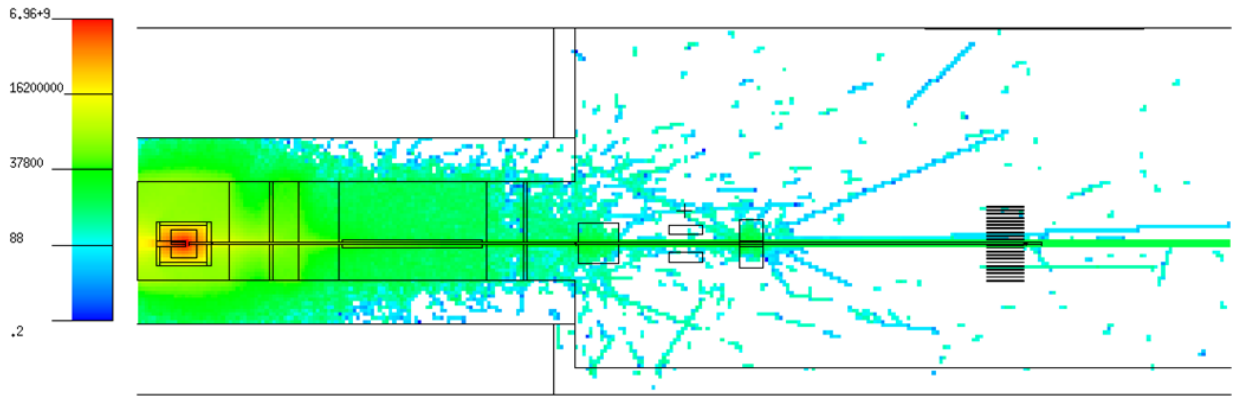

Figure 7: Vertical cross section of the neutron flux calculated for the model. Beam goes from left to right.

The neutron flux on the face of the LH_2/LD_2 cryogenic target (tally #3) is 1.7×10^4 n/(s·cm^2). The spectrum of neutrons at and around the face of the cryogenic target is shown in Fig. 9. The neutron energy on the cryogenic target varied between 0.1 – 1 GeV and flux is not enough to provide a significant background in the case of np or nd interactions in the cryogenic target.

The neutron dose rate for the silicon photomultipliers (SiPM) of the start counter [9, 10, 12] and BCAL [11, 12] is given in Fig. 10 (left). There is an issue for SiPM and low level of BCAL. Previous studies stand that the dose rate of 30 mreh/h increases a dark current at SiPM by a factor of 5 after 75 days of running period [13].

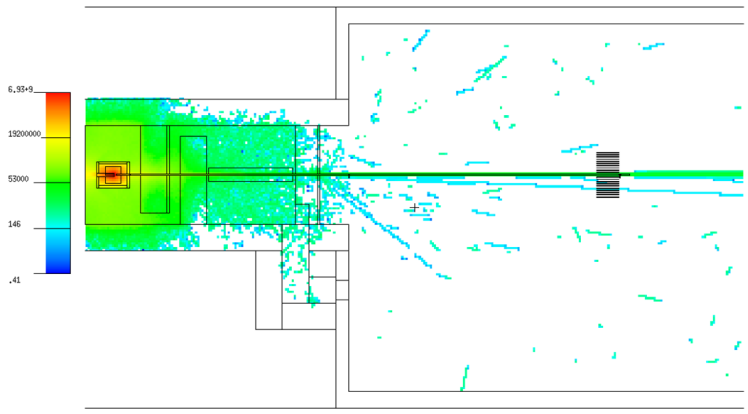

Figure 8: Horizontal cross section of the neutron flux calculated for the model. Beam goes from left to right.

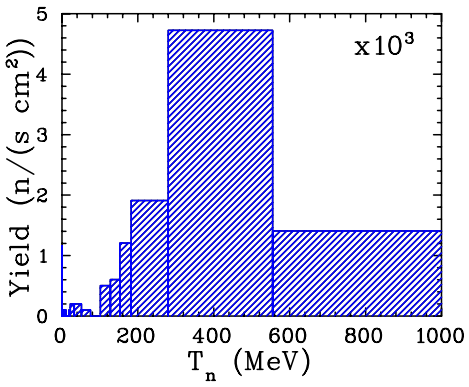

Figure 9: Neutron energy spectrum at the beam and face of the cryogenic target, tally #3.

Table 2: Neutron (2nd column) and gamma (3rd column) background flux calculated for different tallies (1st column) Percentage in brackets shows statistical uncertainties of MC simulations..

Tally	Neutron flux (n/(s·cm^2))	Photon flux (γ/(s·cm^2))
#1	(8.0±0.5)×10^4 (6.7%)	(31.1±0.1)×10^6 (0.3%)
#2	(2.2±1.7)×10^3 (75%)	(3.3±1.0)×10^3 (31%)
#3	(1.7±0.2)×10^4 (11%)	(27.2±0.1)×10^6 (0.3%)
#4	$> 1.7 \times 10^2$	(9.9±1.6)×10^3 (16%)
#20	(236.0±0.1)×10^8(0.1%)	(223.0±0.5)×10^6 (0.02%)
#21	(41.7±0.1)×10^8(0.1%)	(10.7±0.1)×10^6 (0.2%)

In our initial calculations (Fig. 10), we ignored Pair Spectrometer and FM magnets. In new calculations (Table 3), we took them into account as well as 4 SEG-blocks ($132 \times 132 \times 66\ cm^3$) shildings around the beam pipe and a concrete block ($132 \times 132 \times 20\ cm^3$) with a steel collimator for the

Table 3: Neutron (2nd column) and gamma (3rd column) dose rate background calculated for different tallies (1st column). Percentage in brackets shows statistical uncertainties of MC simulations.

Tally	Dose rate (mrem/h)	Dose rate (mrem/h)
#5	0.11±0.04 (36%)	$(2.0\pm0.1)\times10^{-2}$ (3.8%)
#6	632±145 (23%)	$(3.0\pm0.1)\times10^{3}$ (2.9%)
#7	0.02±0.02 (100%)	$(7.1\pm4.2)\times10^{-3}$ (59%)
#8	0.01±0.01 (100%)	$(3.0\pm1.8)\times10^{-3}$ (58%)
#9	> 0.1	$(2.2\pm0.5)\times10^{-2}$ (25%)
#10	1.8±1.8 (100%)	(0.52±0.04) (7.8%)
#11	> 0.1	(0.57±0.10) (18%)
#12	> 0.1	(0.45±0.05) (10%)
#13	0.01±0.01 (100%)	(0.42±0.05) (13%)
#14	0.3±0.3 (86%)	(0.46±0.05) (11%)
#15	0.4±0.2 (61%)	(0.36±0.04) (11%)
#16	0.1±0.1 (91%)	(0.28±0.02) (7.4%)
#17	1.2±0.8 (66%)	(0.24±0.01) (5.5%)
#18	0.3±0.2 (77%)	(0.19±0.01) (3.4%)
#19	0.3±0.2 (57%)	(0.18±0.01) (4.0%)

beam pipe (outer ∅13 cm and inner ∅8 cm). We are confident that the additional steel collimator between SEG-blocks reduces a neutron radiation dose for BCAL up to >0.1 mrem/h (tallies #10 – #19) (Table 3) which is negligible. While there is still an issue for SiPMs of the start counter which is 632±145 rem/h (tally #6). SiPMs can be replaced with regular PMTs, but we have to worry about shielding the magnetic field. Another option is MCP-PMTs which are rad hard and resistant to magnetic fields.

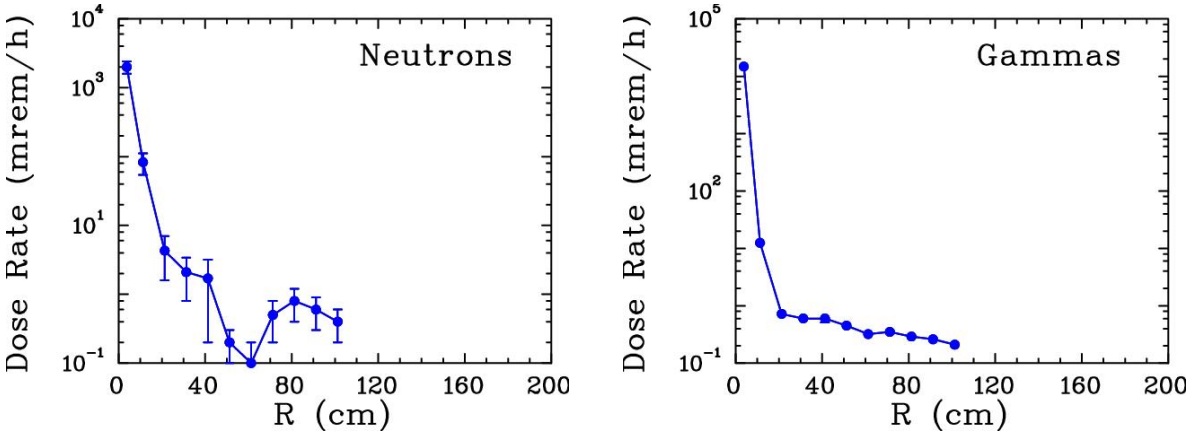

Figure 10: Neutron (left) and gamma (right) dose rate background calculated for SipM (tally #6) and BCAL (tallies #10-19) on the face of the cryogenic target. In this case, we did not take into account additional shildings in the experimental hall.

The neutron energy on the cryogenic target varied between 0.1 – 1 GeV and flux is low enough to provide a significant background in the case of np or nd interactions in the cryogenic target (Fig. 9).

To summarize, the neutron flux and dose rate for the KLF experiment is below the RadCon limit as Tables 2 and 3 show. Overall, the Be-target assembly conceptual design satisfies the RadCon requirement establishing the radiation dose rate limit in the Hall. The full engineering design is in progress.

3.2 Gamma Background

To estimate the photon flux in a beam and gamma dose rate in the experimental Hall D from scattered neutrons, we used the same MCNP Transport code [2]. After passing through 30 R.L. tungsten beam plug and the charged background component removed by the sweep magnet, we will have some residual γ background produced by EM showers. The vertical cross section of the gamma flux is given in Fig. 11. The energy spectrum of residual γs is shown in Fig. 12. It decreases exponentially with increasing energy of photons and cannot exceed 30 MeV. The gamma dose calculated for the layout from Fig. 7 on tally #5 is $(2.0\pm0.1)\times10^{-2}$ mrem/h which is acceptable by RadCon.

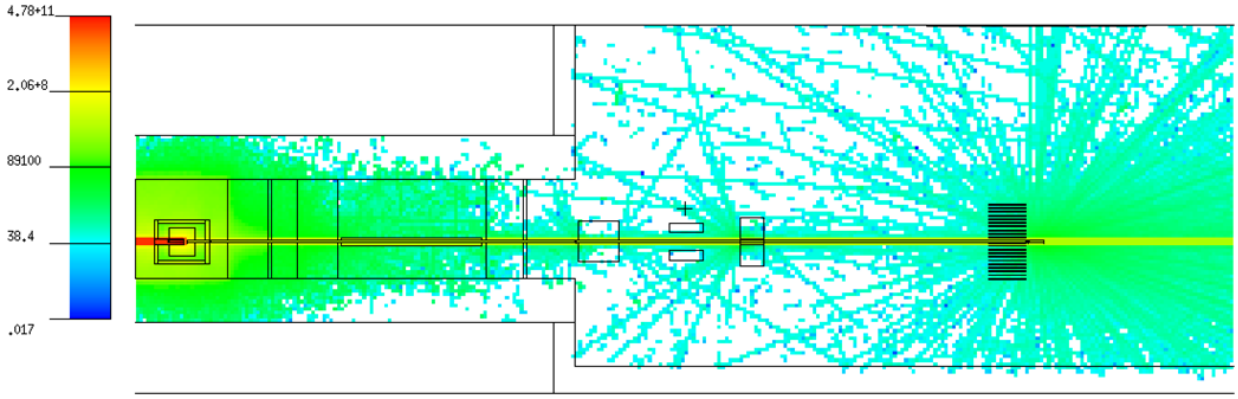

Figure 11: Vertical cross section of the gamma flux calculated for the model. Beam goes from left to right.

The gamma dose rate (Table 3) (Fig. 10 (right)) which is acceptable for the silicon photomultipliers (SiPM) [9, 10, 12] and BCAL [11, 12] as well.

To summarize, the photon flux and dose rate for the KLF experiment is tolerable (Tables 2 and 3).

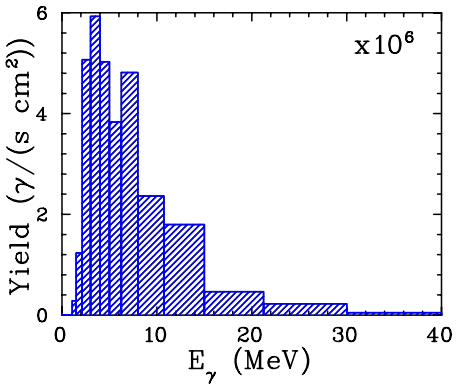

Figure 12: Gamma energy spectrum on the beam and face of the cryogenic target, tally #1.

4 Acknowledgements

The authors are grateful to Eugene Chudakov for many useful communications and discussions and to Stephanie Worthington for details of the geometry of the collimator cave. This material is based upon work supported by the U.S. Department of Energy, Office of Science, Office of Nuclear Physics, under Award Number DE–SC0016583.

5 Appendix: Geometry of the Collimator Cave

Schematic view of the collimator cave with the Be-target assemply is given for z- (Fig. 13), x- (Fig. 14), and y-dimension (Fig. 15), respectively.

References

[1] M. J. Amaryan, M. Bashkanov, J. Ritman, J. R. Stevens, I. Strakovsky *et al.* [GlueX Collaboration], arXiv:1707.05284 [hep-ex].

[2] T. Goorley *et al.*, Nucl. Tech. **180**, 298. (2012); https://mcnp.lanl.gov/ .

[3] GlueX wiki: https://halldweb.jlab.org/wiki/images/d/df/CollimatorElevationSept08.png ; S. Worthington, private communication, 2018..

[4] M. Bashkanov *et al.*, *Flux monitor memo*.

[5] F. Barbosa, C. Hutton, A. Sitnikov, A. Somov, S. Somov, and I. Tolstukhin, Nucl. Instrum. Meth. A **795**, 376 (2015).

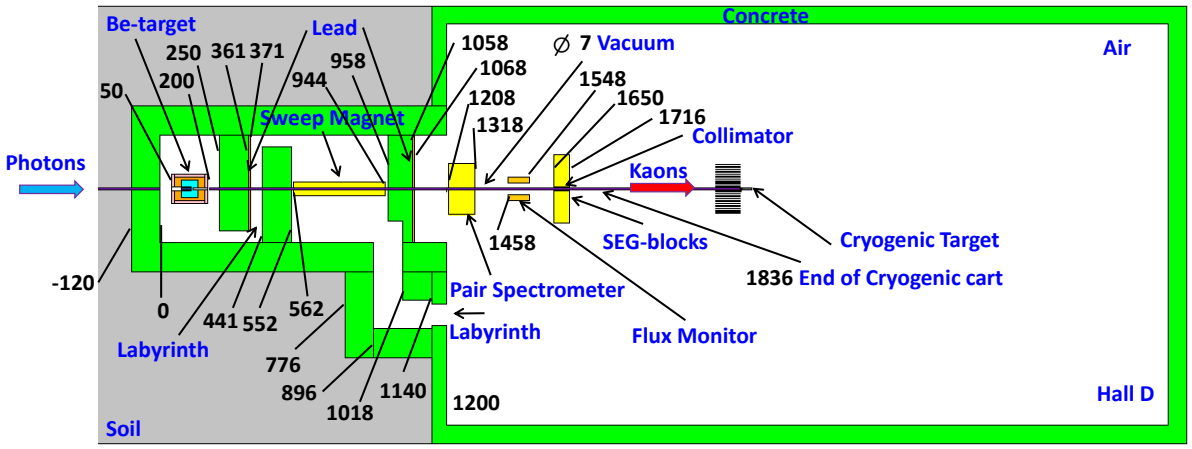

Figure 13: Schematic view of the collimator cave with the Be-target assemply: z-dimension (in cm units). Beam goes from left to right.

[6] A. D. Brody *et al.*, Phys. Rev. Lett. **22**, 966 (1969).

[7] M. G. Albrow *et al.*, Nucl. Phys. B **23**, 509 (1970).

[8] ICRP 116 Publication, *Conversion Coefficients for Radiological Protection Quantities for External Radiation Exposures*, Annals of the ICRP, **40**, No 2-5 (2010).

[9] Y. Qiang, C. Zorn, F. Barbosa, and E. Smith, Nucl. Instrum. Meth. A **698**, 234 (2013).

[10] E. Pooser, F. Barbosa, W. Boeglin, C. Hutton, M. Ito, M. Kamel, P. Khetarpal, A. LLodra, N. Sandoval, S. Taylor, C. Yero, T. Whitlatch, S. Worthington, and B. Zihlmann, to be submitted to Nucl. Instrum. Meth. A.

[11] T. D. Beattie *et al.*, Nucl. Instrum. Meth. A **896**, 24 (2018).

[12] P. Degtiarenko, A. Fass, G. Kharashvili, and A. Somov, Preprint JLAB-TN-11-005, 2011.

[13] A. Somov, Preprint GlueX–doc–1646, 2011.

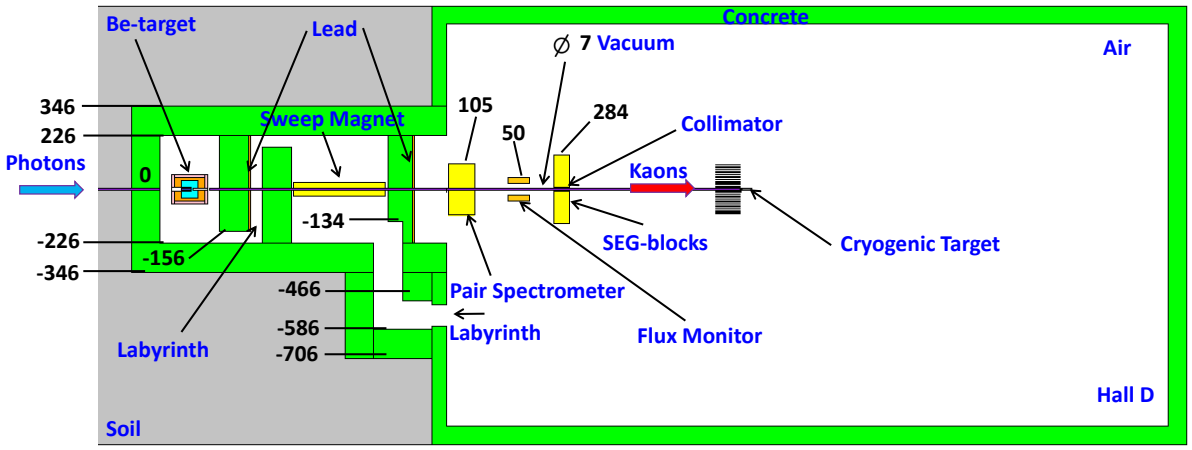

Figure 14: Schematic view of the collimator cave with the Be-target assemply: x-dimension (in cm units). Beam goes from left to right.

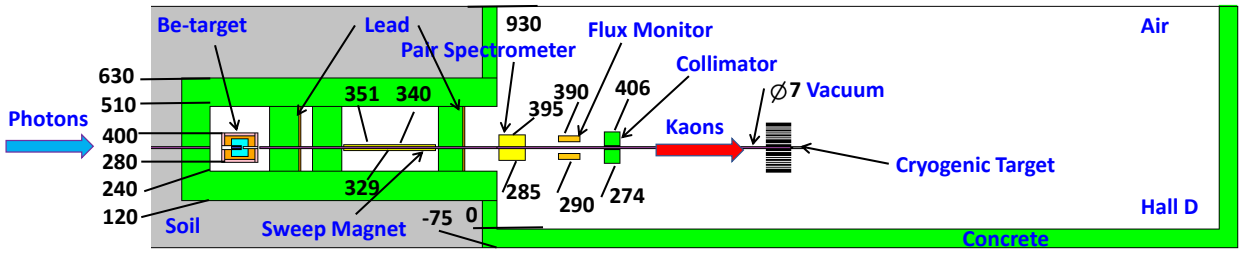

Figure 15: Schematic view of the collimator cave with the Be-target assemply: y-dimension (in cm units). Beam goes from left to right.